Engineering with Computers
https://doi.org/10.1007/s00366-021-01475-8

ORIGINAL ARTICLE

The role of spatial variation of the nonlocal parameter on the free vibration of functionally graded sandwich nanoplates

Pham Van Vinh[1] · **Abdelouahed Tounsi**[2,3,4]

Received: 22 May 2021 / Accepted: 5 July 2021

Abstract
The role of the spatial variation of the nonlocal parameter on the free vibration of functionally graded sandwich nanoplates is investigated in this study. The key achievement of this work is that the classical nonlocal elasticity theory is modified to take into account the dependence of nonlocal parameters on the varying of materials through the thickness of the functionally graded sandwich nanoplates. Hamilton's principle is adopted to establish the governing equations of motion using a new inverse hyperbolic shear deformation theory. Numerical results are carried out via Navier's solution for the fully simply supported rectangular functionally graded sandwich nanoplates, and they are compared with the available results to confirm the accuracy and efficiency of the proposed algorithm. Besides, the effects of some parameters such as the spatial variation of the nonlocal parameters, the aspect ratio, the side-to-thickness ratio as well as the power-law index on the free vibration of the nanoplates are also investigated cautiously. The results show that the variation of the nonlocal parameters plays a significant role in the free vibration of the functionally graded sandwich nanoplates, which is never investigated in the literature. The present methodology could be applied to the design and application of the micro/nanostructures.

Keywords Functionally graded materials · Sandwich nanoplates · Inverse hyperbolic shear deformation theory · Nonlocal elasticity theory · Spatial variation of the nonlocal parameter · Free vibration analysis

1 Introduction

Recently, the consumption of micro/nanostructures is increasing in exponential principle in many fields of engineering and technology, some remarkable examples can be expressed here are solar cells energy, micro/nanosensors, biological applications as well as micro/nanoelectromechanical systems (MEMS/NEMS), and so on. In these cases, the behaviors of the nanoplates, nanobeams, and nanoshells are completely different from those of the macrostructures. The reason is that the effect of small-scale length parameter on the behavior of micro/nanostructures is very essential. Hence, it is necessary to have an excellent understanding of the mechanical and thermal behavior of micro/nanostructures. Many methods have been introduced to study the static, dynamic, as well as thermal behavior of the micro/nanostructures. For example, atomistic simulations and experimental methods are the most accurate methods that can predict and capture very well the small-scale effects. However, the atomistic simulations cost a lot of time and computer computation, and the experimental methods cost much time and economy. As a consequence, many continuum mechanics theories have been developed to evaluate the behavior of the micro/nanostructures. Several noticeable theories can be presented here are modified couple stress theory (MCST) [1, 2], the surface elasticity theory (SET) [3–8], the strain gradient theory (SGT) [9, 10] and nonlocal strain gradient (NSGT) [11, 12], the micropolar and nonlocal polar theory [13, 14], and nonlocal elasticity theory (NET) [15, 16]. The NET has been applied to study dynamic, static, as well as thermomechanical behavior of

✉ Pham Van Vinh
phamvanvinh@lqdtu.edu.vn

[1] Department of Solid Mechanics, Le Quy Don Technical University, 236 Hoang Quoc Viet, Hanoi, Vietnam

[2] YFL (Yonsei Frontier Lab), Yonsei University, Seoul, South Korea

[3] Department of Civil and Environmental Engineering, King Fahd University of Petroleum & Minerals, Dhahran 31261, Eastern Province, Saudi Arabia

[4] Material and Hydrology Laboratory, Civil Engineering Department, Faculty of Technology, University of Sidi Bel Abbes, Sidi Bel Abbès, Algeria

micro/nanostructures in numerous published works. For instance, Reddy et al. [17, 18] employed NET to investigate the bending, buckling, and vibration of nanobeams and carbon nanotubes. Ebrahimi et al. [19] studied the vibration of piezoelectric nanobeams using NET. Thai et al. [20] applied sinusoidal shear deformation beam theory in combination with NET to examine the bending, buckling, and free vibration of nanobeams. The linear and nonlinear free vibration of functionally graded (FG) nanobeams have been investigated by Eltaher et al. [21] and Nazemezhad et al. [22]. A combination of NET and MCST was developed by Ebrahimi [23] to analyze the static stability and vibration of nonlocal microstructures-dependent nanostructures with the application of Chebyshev–Ritz method. Hadji et al. [24] applied nonlocal hyperbolic shear deformation beam theory to analyze free vibration of porous FG nanobeams. Youcef et al. [25] applied the nonlocal shear deformation and energy principle to analyze the free vibration of porous FG nanobeams. Shariati et al. [26] employed the NET and Laplace transformation to study dynamic response of axially FG nanobeams. Zenkour [27] studied the thermoelastic vibration of nanoplates using a novel mixed formulation of NET. Aghababaei et al. [28] used NET in cooperation with third-order shear deformation theory (TSDT) to analyze the bending and free vibration of nanoplates. A Levy-type solution for free vibration and buckling analysis of nanoplates using NET has been carried out by Aksencer and his coworkers [29]. Hosseini-Hashemi et al. [30] developed an exact solution for free vibration analysis of FG circular/annular Mindlin nanoplates using NET. Zare et al. [31] investigated the free vibration of FG rectangular nanoplates with arbitrary boundary conditions using NET and an analytical solution. Several works on the bending, free vibration, and buckling of orthotropic, FG nanoplates have been carried out by Sobhy et al. [32–34]. A novel nonlocal single variable shear deformation theory has been developed by Hoa et al. [35] to investigate the bending and free vibration of FG nanoplates. Akbas [36] studied modal behavior of viscoelastic nanorods under an axially harmonic load. Ghandourah et al. [37] analyzed dynamic response of the FG nanobeams with different porosity models. Natarajan et al. [38] studied the flexural free vibration of FG nanoplates using Eringen's differential form of NET and isogeometric-based finite-element method.

To achieve some delightful features and high-performance applications in micro/nanostructures, functionally graded materials (FGMs) have been widely applied to produce these structures. These materials are first introduced by some Japanese researchers in 1984 (Koizumi [39]) and have been applied widely in some fields of engineering and technology. Hence, the investigation on the static, dynamic, and buckling behavior of single-layer and sandwich FG structures has been carried out by numerous researchers (Swaminathan et al. [40], Sayyad et al. [41], Thom et al. [42], Vinh et al. [43], Abouelregal et al. [44], Civalek et al. [45], Lyashenko et al. [46], and Daikh et al. [47]). For instance, Nguyen et al. [48] studied the vibration and buckling behavior of functionally graded sandwich (FGSW) plates using first-order shear deformation theory (FSDT) with an improvement of transverse shear stiffness. Vinh [49] developed a new mixed four-node quadrilateral plate element based on FSDT to analyze the static bending of variable thickness FG plates. Hassan et al. [50] studied the relations between the various critical temperatures of thin FG plates. AlSaid-Alwan et al. [51] used different types of beam theories to analyze the free vibration of the FG beams. Hadji et al. [52, 53] analyzed free vibration of porous FG and FGSW plates under various boundary conditions. A comprehensive study on the buckling and free vibration of FGSW plates has been done by Zenkour [54] using sinusoidal shear deformation theory (SSDT). Tahir et al. [55] studied wave propagation of ceramic–metal FGSW plates with different porosity distributions in hygro-thermal environment. Rebai et al. [56] analyzed thermoelastic response of FGSW plates via a simple integral HSDT. Bennoun et al. [57] developed a novel five-variable refined plate theory to analyze free vibration of FGSW plates. Meiche et al. [58] studied buckling and free vibration of FGSW plates using a new hyperbolic shear deformation theory (HySDT). A new inverse trigonometric shear deformation theory (iTrSDT) had been developed by Nguyen et al. [59] to study the static bending, free vibration, and buckling of FGSW plates. Bessaim et al. [60] developed a new HSDT with hyperbolic distribution shape function to take into account the hyperbolic distribution of the transverse shear strain through the thickness of the plates. Pham et al. [61] developed a combination of a new hyperbolic shear deformation theory and finite-element method to study the static bending of FGSW plates. To consider the thickness stretching effects, some quasi-3D theories have been developed by Neves et al. [62], Natarajan et al. [63], and some of their references. Vinh [64] studied deflections, stresses, and free vibration of FGSW plates using a hybrid quasi-3D theory. A three-dimensional vibration of FGSW plates had been investigated by Li et al. [65] via three-dimensional linear elasticity theory. Iurlaro et al. [66] established a refined Zigzag theory for analysis the bending and free vibration analysis of the FGSW plates. For micro/nanostructures, Arefi et al. [67] used Kirchhoff plate theory and NET to study the size-dependent free vibration and dynamic response of piezo-electro-magnetic sandwich nanoplates resting on the viscoelastic foundation. In the other work of Arefi et al. [68], the nonlocal SGT was applied to analyze the magneto-electro-elastic vibration of FG-core sandwich and piezomagnetic face sheets resting on elastic foundation. Zeng et al. [69] studied the nonlinear vibration of piezoelectric sandwich nanoplates with FG porous core and piezoelectric face sheets. Daikh et al. [70] studied vibration of FGSW nanoplates in the thermal environment using NET and HSDT.

It can be seen that in the most of the above studies, the NET has been applied to analyze the FG and FGSW nanoplates with an assumption of a constant nonlocal parameter through the

thickness direction. However, according to several recent works on the analysis of micro/nanostructures such as Salehipour et al. [71] and Batra [72], the nonlocal parameter is a material-dependent property. It means that the nonlocal parameter varies through the thickness of the FG and FGSW nanoplates. Besides, the study on the free vibration of FGSW nanoplates is still limited. According to these comments, it is necessary to analyze free vibration of FGSW nanoplates via NET with the material-dependent nonlocal parameters. It is the main goal of this study to modify the NET to take into account for the spatial variation of the nonlocal parameters for free vibration analyze of the FG nanoplates. The frameworks of the paper are as follows: Sect. 2 gives the construction of three types of FGSW nanoplates and the basic formulations of the problem. Section 3 gives several comparison studies to verify the accuracy of the proposed algorithm in some special cases, and then, several deep investigations on the role of the spatial variation of the nonlocal parameter as well as the effects of some parameters on the free vibration of the FGSW nanoplates are carried out cautiously. Section 4 gives some remarkable conclusions and some potential suggestions for future work on the analysis of the FG and FGSW micro/nanostructures.

2 The theoretical formulation and solution algorithm

2.1 Functionally graded sandwich nanoplates

In this study, three types of functionally graded sandwich (FGSW) nanoplates, namely "Type A", "Type B", and "Type C" are considered. The FGSW nanoplates of type A consist of one FG core, one homogenous metal face sheet at the bottom layer, and one homogenous ceramic face sheet at top layer. The FGSW nanoplates of type B consist of one homogenous ceramic core and two FG face sheets. The FGSW nanoplates of type C consist of one homogenous metal core and two layers made of FG materials. The geometry and dimensions of the sandwich nanoplates are demonstrated in Fig. 1. In which the variables h_0, h_1, h_2, and h_3 are used to denote the coordinates of the surfaces of the bottom, core, and top layers.

2.1.1 The FGSW nanoplates of type A

The variation of the effective material properties through the thickness of the FGSW nanoplates of type A is obtained by the following formulae:

$$\begin{cases} P(z) = P_{\mathrm{m}} & h_0 \le z \le h_1 \\ P(z) = P_{\mathrm{m}} + \left(P_{\mathrm{c}} - P_{\mathrm{m}}\right)\left(\frac{z-h_1}{h_2-h_1}\right)^p & h_1 < z < h_2 \\ P(z) = P_{\mathrm{c}} & h_2 \le z \le h_3 \end{cases}, \tag{1}$$

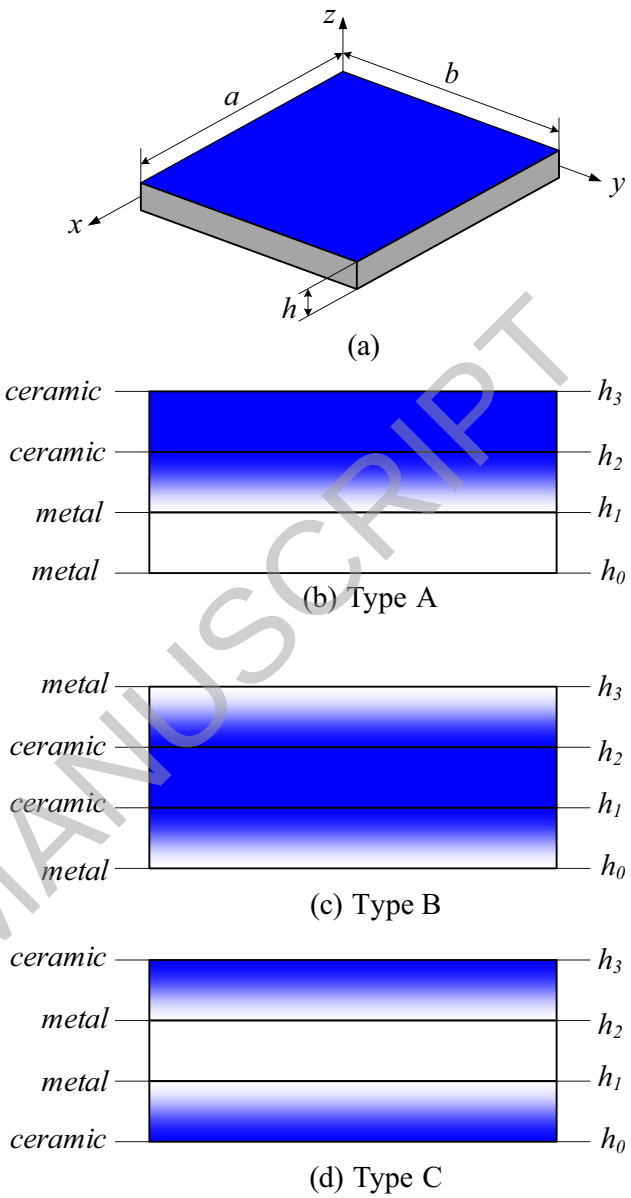

Fig. 1 The geometry and construction of functionally graded sandwich nanoplates

where P_{c}, P_{m} are the material properties of the ceramic and metal components, respectively.

2.1.2 The FGSW nanoplates of type B

For the FGSW nanoplates of type B, the material properties of the materials through the thickness of the plates are calculated by

$$\begin{cases} P(z) = P_m + (P_c - P_m)\left(\frac{z-h_0}{h_1-h_0}\right)^p & h_0 \le z \le h_1 \\ P(z) = P_c & h_1 < z < h_2 \\ P(z) = P_m + (P_c - P_m)\left(\frac{z-h_3}{h_2-h_3}\right)^p & h_2 \le z \le h_3 \end{cases}. \quad (2)$$

2.1.3 The FGSW nanoplates of type C

In the cases of FGSW nanoplates of type C, the following formulas are used to evaluate the material properties of the materials:

$$\begin{cases} P(z) = P_c + (P_m - P_c)\left(\frac{z-h_0}{h_1-h_0}\right)^p & h_0 \le z \le h_1 \\ P(z) = P_m & h_1 < z < h_2 \\ P(z) = P_c + (P_m - P_c)\left(\frac{z-h_3}{h_2-h_3}\right)^p & h_2 \le z \le h_3 \end{cases}. \quad (3)$$

The material properties of several individual materials are presented in Table 1 (Natarajan [38], Zenkour [54]).

The FGSW nanoplates which are investigated in this work are made of Al as metal component and Al_2O_3 as ceramic component. The variation of the effective Young's modulus through the thickness of the FGSW nanoplates with three types of sandwich nanoplates are demonstrated in Fig. 2.

2.2 A new inverse hyperbolic shear deformation theory

2.2.1 Kinematic

In this study, a new inverse hyperbolic shear deformation theory (IHSDT) is developed to investigate the free vibration of the FGSW nanoplates. The displacement of the proposed IHSDT is written as follows:

$$\begin{aligned} u(x,y,z,t) &= u(x,y,t) - z\frac{\partial w(x,y,t)}{\partial x} + f(z)\varphi_x(x,y,t) \\ v(x,y,z,t) &= v(x,y,t) - z\frac{\partial w(x,y,t)}{\partial y} + f(z)\varphi_y(x,y,t) \\ w(x,y,z,t) &= w(x,y,t), \end{aligned} \quad (4)$$

Table 1 The material properties of several individual materials

Material constants	Materials			
	Al_2O_3	Si_3N_4	Al	SUS304
E (GPa)	380	348.43	70	201.04
ρ (kg/m^3)	3800	2370	2707	8166
ν	0.3	0.3	0.3	0.3

where $f(z)$ is the distribution shape function, which is given by

$$f(z) = \Gamma \cdot \sinh^{-1}\left(\frac{z}{\pi h}\right) + \Theta \cdot \tanh^{-1}\left(\frac{z}{\pi h}\right), \quad (5)$$

with

$$\Gamma = \frac{5\pi^3 h\sqrt{\frac{1}{4\pi^2}+1}}{4\pi^2\sqrt{\frac{1}{4\pi^2}+1} - 4\pi^2 + 1}, \Theta = \frac{5\pi h\left(1-4\pi^2\right)}{4\left(4\pi^2\sqrt{\frac{1}{4\pi^2}+1} - 4\pi^2 + 1\right)}. \quad (6)$$

The shear strain shape functions are chosen to satisfy the condition of the free transverse shear stresses on two surfaces of the plates and the nonlinear distribution through the thickness. Therefore, the proposed IHSDT does not need any shear correction factor. Additionally, the two coefficients Γ and Θ are calculated in such a way that the proposed theory allows for realistic prediction of the displacements and stress distribution through the thickness of the plates by comparing the results of the present theory and available results of three-dimensional elasticity solutions. The strain fields of the plate are obtained as

$$\begin{aligned} \varepsilon_x &= \frac{\partial u}{\partial x} - z\frac{\partial^2 w}{\partial x^2} + f(z)\frac{\partial \varphi_x}{\partial x} \\ \varepsilon_y &= \frac{\partial v}{\partial y} - z\frac{\partial^2 w}{\partial y^2} + f(z)\frac{\partial \varphi_y}{\partial y} \\ \gamma_{xy} &= \frac{\partial u}{\partial y} + \frac{\partial v}{\partial x} - 2z\frac{\partial^2 w}{\partial x \partial y} + f(z)\left(\frac{\partial \varphi_x}{\partial y} + \frac{\partial \varphi_y}{\partial x}\right) \\ \gamma_{xz} &= g(z)\varphi_x \\ \gamma_{yz} &= g(z)\varphi_y, \end{aligned} \quad (7)$$

where $g(z) = f'(z)$. In the matrix form

$$\begin{Bmatrix} \varepsilon_x \\ \varepsilon_y \\ \gamma_{xy} \end{Bmatrix} = \begin{Bmatrix} \varepsilon_x^0 \\ \varepsilon_y^0 \\ \gamma_{xy}^0 \end{Bmatrix} + z\begin{Bmatrix} \varepsilon_x^1 \\ \varepsilon_y^1 \\ \gamma_{xy}^1 \end{Bmatrix} + f(z)\begin{Bmatrix} \varepsilon_x^2 \\ \varepsilon_y^2 \\ \gamma_{xy}^2 \end{Bmatrix}, \begin{Bmatrix} \gamma_{xz} \\ \gamma_{yz} \end{Bmatrix} = g(z)\begin{Bmatrix} \gamma_{xz}^0 \\ \gamma_{yz}^0 \end{Bmatrix}. \quad (8)$$

In which

$$\begin{Bmatrix} \varepsilon_x^0 \\ \varepsilon_y^0 \\ \gamma_{xy}^0 \end{Bmatrix} = \begin{Bmatrix} \frac{\partial u}{\partial x} \\ \frac{\partial v}{\partial y} \\ \frac{\partial u}{\partial y} + \frac{\partial v}{\partial x} \end{Bmatrix}, \begin{Bmatrix} \varepsilon_x^1 \\ \varepsilon_y^1 \\ \gamma_{xy}^1 \end{Bmatrix} = -\begin{Bmatrix} \frac{\partial^2 w}{\partial x^2} \\ \frac{\partial^2 w}{\partial y^2} \\ 2\frac{\partial^2 w}{\partial x \partial y} \end{Bmatrix}, \begin{Bmatrix} \varepsilon_x^2 \\ \varepsilon_y^2 \\ \gamma_{xy}^2 \end{Bmatrix} = \begin{Bmatrix} \frac{\partial \varphi_x}{\partial x} \\ \frac{\partial \varphi_y}{\partial y} \\ \frac{\partial \varphi_x}{\partial y} + \frac{\partial \varphi_y}{\partial x} \end{Bmatrix}, \begin{Bmatrix} \gamma_{xz}^0 \\ \gamma_{yz}^0 \end{Bmatrix} = \begin{Bmatrix} \varphi_x \\ \varphi_y \end{Bmatrix}. \quad (9)$$

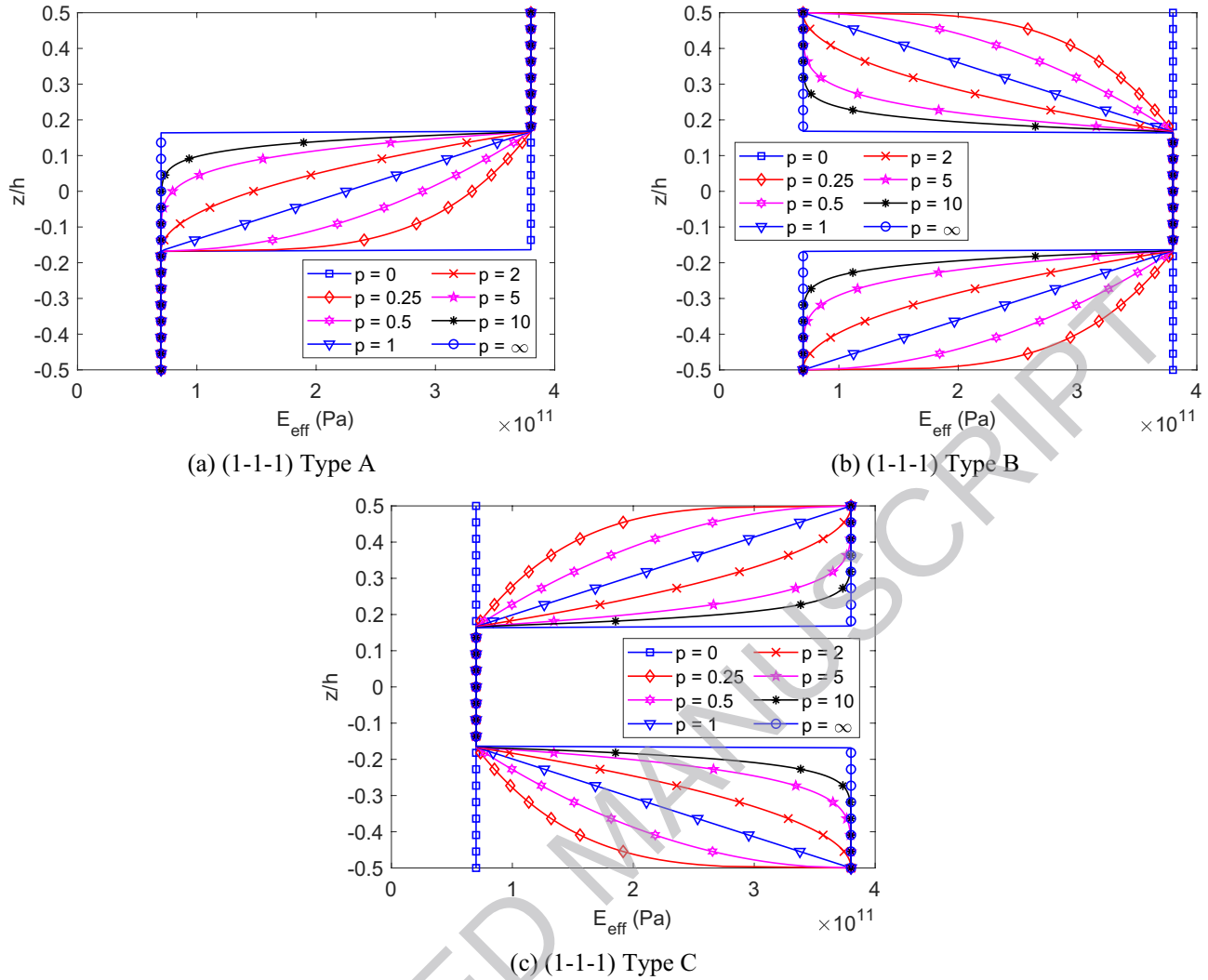

(a) (1-1-1) Type A

(b) (1-1-1) Type B

(c) (1-1-1) Type C

Fig. 2 The variation of effective Young's modulus through the thickness of the Al_2O_3/Al FGSW nanoplates

2.2.2 Constitutive relations

The constitutive equation of the plate is expressed as

$$\begin{Bmatrix} \sigma_x \\ \sigma_y \\ \tau_{xy} \\ \tau_{yz} \\ \tau_{xz} \end{Bmatrix}^{(n)} = \begin{bmatrix} C_{11} & C_{12} & 0 & 0 & 0 \\ C_{12} & C_{22} & 0 & 0 & 0 \\ 0 & 0 & C_{66} & 0 & 0 \\ 0 & 0 & 0 & C_{44} & 0 \\ 0 & 0 & 0 & 0 & C_{55} \end{bmatrix}^{(n)} \begin{Bmatrix} \varepsilon_x \\ \varepsilon_y \\ \gamma_{xy} \\ \gamma_{yz} \\ \gamma_{xz} \end{Bmatrix}^{(n)}, \tag{10}$$

where

$$C_{11} = C_{22} = \frac{E(z)}{1-\nu^2},\ C_{12} = \frac{\nu E(z)}{1-\nu^2},\ C_{44} = C_{55} = C_{66} = \frac{E(z)}{2(1+\nu)}. \tag{11}$$

2.3 The nonlocal elasticity theory

To take into account the small-scale effects on the behavior of the nanostructures, Eringen [15, 16] introduced a nonlocal elasticity theory in both integral and differential form. In the nonlocal elasticity theory, the stress at any point depends on the strains at all neighbor points in the continuum body. The differential form of nonlocal elasticity theory is usually used by many researchers, whereas the nonlocal parameter does not depend on the variation of materials. The differential form of the nonlocal elasticity theory [16] is given by the following formula:

$$\left(1-\mu\nabla^2\right)\sigma_{ij} = s_{ij}, \tag{12}$$

where σ_{ij}, s_{ij} are, respectively, the nonlocal and local stress tensors, $\nabla^2 = \partial^2/\partial x^2 + \partial^2/\partial y^2$ is the second Laplace operator, $\mu = (e_0 a)^2$ (nm^2) is the nonlocal parameter, in which e_0 is a material constant which is determined via experimental or atomistic dynamic for each material, and a is an internal characteristic length which relates to the distance of the molecules, lattice parameter, and granular size. Some studies show that the nonlocal parameter is not constant with the variation of materials and the dimensions of the structures (Salehipour [71], Batra [72]). In this study, the nonlocal parameter is assumed to change as other material properties of functionally graded materials. Therefore, the nonlocal parameter at any point of the FGSW nanoplates is calculated via Eqs. (1)–(3) as a function of z-coordinates depending on the type of the sandwich plates.

Hence, the nonlocal constitutive relations of the plates can be expressed as follows:

$$\begin{aligned}\begin{Bmatrix} s_x \\ s_y \\ s_{xy} \\ s_{yz} \\ s_{xz} \end{Bmatrix}^{(n)} &= \begin{Bmatrix} \sigma_x \\ \sigma_y \\ \tau_{xy} \\ \tau_{yz} \\ \tau_{xz} \end{Bmatrix}^{(n)} - \mu(z)\nabla^2 \begin{Bmatrix} \sigma_x \\ \sigma_y \\ \tau_{xy} \\ \tau_{yz} \\ \tau_{xz} \end{Bmatrix}^{(n)} \\ &= \begin{bmatrix} C_{11} & C_{12} & 0 & 0 & 0 \\ C_{12} & C_{22} & 0 & 0 & 0 \\ 0 & 0 & C_{66} & 0 & 0 \\ 0 & 0 & 0 & C_{44} & 0 \\ 0 & 0 & 0 & 0 & C_{55} \end{bmatrix}^{(n)} \begin{Bmatrix} \varepsilon_x \\ \varepsilon_y \\ \gamma_{xy} \\ \gamma_{yz} \\ \gamma_{xz} \end{Bmatrix}^{(n)}. \end{aligned} \tag{13}$$

It is obvious that the present nonlocal constitutive relations of the FGSW nanoplates using the present nonlocal elasticity theory are completely different to the classical Eringen's nonlocal elasticity theory. In Eringen's nonlocal elasticity theory, the effects of the nonlocal parameter are similar at any thickness coordinate, because the nonlocal parameter is constant through the thickness of the FGSW nanoplates. On the contrary, the effects of the nonlocal parameter are different across the thickness directions of the FG nanoplates. From Eq. (13), it is obvious that the relation between the nonlocal stress σ_{ij} and the local strain ε_{ij} not only depends on the variation of Young's modulus and the Poisson's ratio but also depends on the variation of the nonlocal parameter through the z-direction. When the exact nonlocal parameters of the individual material are determined, the current methodology can be applied to generate more accurate results for design and applications of the FG micro/nanostructures.

2.4 The governing equations of motion

The equations of motion are achieved via Hamilton's principle

$$0 = \int_0^T (\delta\Pi - \delta T)\mathrm{d}t, \tag{14}$$

where $\delta\Pi$ is the variation of the strain energy and δT is the variation of the kinematic energy of the plates. The variation of the strain energy is obtained as the following expression:

$$\delta\Pi = \int_V \left(\sigma_x\delta\varepsilon_x + \sigma_y\delta\varepsilon_y + \tau_{xy}\delta\varepsilon_{xy} + \tau_{xz}\delta\varepsilon_{xz} + \tau_{yz}\delta\varepsilon_{yz}\right)\mathrm{d}V. \tag{15}$$

The variation of the kinetic energy of the plate is expressed as

$$\delta T = \int_V (\dot{u}\delta\dot{u} + \dot{v}\delta\dot{v} + \dot{w}\delta\dot{w})\rho(z)\mathrm{d}V. \tag{16}$$

Substituting Eqs. (7) and (10) into Eq. (15), substituting Eq. (4) into Eq. (16), and considering the nonlocal relations of Eq. (12), after integrating through the thickness of the plates, the governing equations of motion of the sandwich plates are derived from Eq. (14) as the following formulae:

$$\begin{aligned}
\delta u &: \frac{\partial N_x}{\partial x} + \frac{\partial N_{xy}}{\partial y} = I_0\ddot{u} - I_1\frac{\partial \ddot{w}}{\partial x} + I_2\ddot{\varphi}_x - \nabla^2\left(Y_0\ddot{u} - Y_1\frac{\partial \ddot{w}}{\partial x} + Y_2\ddot{\varphi}_x\right) \\
\delta v &: \frac{\partial N_y}{\partial y} + \frac{\partial N_{xy}}{\partial x} = I_0\ddot{v} - I_1\frac{\partial \ddot{w}}{\partial y} + I_2\ddot{\varphi}_y - \nabla^2\left(Y_0\ddot{v} - Y_1\frac{\partial \ddot{w}}{\partial y} + Y_2\ddot{\varphi}_y\right) \\
\delta w &: \frac{\partial^2 M_x}{\partial x^2} + 2\frac{\partial^2 M_{xy}}{\partial x\partial y} + \frac{\partial^2 M_y}{\partial y^2} = I_0\ddot{w} + I_1\left(\frac{\partial \ddot{u}}{\partial x} + \frac{\partial \ddot{v}}{\partial y}\right) - I_3\left(\frac{\partial^2 \ddot{w}}{\partial x^2} + \frac{\partial^2 \ddot{w}}{\partial y^2}\right) + I_4\left(\frac{\partial \ddot{\varphi}_x}{\partial x} + \frac{\partial \ddot{\varphi}_y}{\partial y}\right) \\
&\qquad - \nabla^2\left[Y_0\ddot{w} + Y_1\left(\frac{\partial \ddot{u}}{\partial x} + \frac{\partial \ddot{v}}{\partial y}\right) - Y_3\left(\frac{\partial^2 \ddot{w}}{\partial x^2} + \frac{\partial^2 \ddot{w}}{\partial y^2}\right) + Y_4\left(\frac{\partial \ddot{\varphi}_x}{\partial x} + \frac{\partial \ddot{\varphi}_y}{\partial y}\right)\right] \\
\delta\varphi_x &: \frac{\partial P_x}{\partial x} + \frac{\partial P_{xy}}{\partial y} - Q_x = I_2\ddot{u} - I_4\frac{\partial \ddot{w}}{\partial x} + I_5\ddot{\varphi}_x - \nabla^2\left(Y_2\ddot{u} - Y_4\frac{\partial \ddot{w}}{\partial x} + Y_5\ddot{\varphi}_x\right) \\
\delta\varphi_y &: \frac{\partial P_y}{\partial y} + \frac{\partial P_{xy}}{\partial x} - Q_y = I_2\ddot{v} - I_4\frac{\partial \ddot{w}}{\partial y} + I_5\ddot{\varphi}_y - \nabla^2\left(Y_2\ddot{v} - Y_4\frac{\partial \ddot{w}}{\partial y} + Y_5\ddot{\varphi}_y\right),
\end{aligned} \tag{17}$$

where N_i, M_i, P_i, and Q_i are the local stress resultants which are calculated by

$$\begin{aligned}
\left(N_x, N_y, N_{xy}\right) &= \sum_{n=1}^{3} \int_{h_{n-1}}^{h_n} \left(s_x,\ s_y,\ s_{xy}\right)^{(n)} \mathrm{d}z \\
\left(M_x, M_y, M_{xy}\right) &= \sum_{n=1}^{3} \int_{h_{n-1}}^{h_n} \left(s_x,\ s_y,\ s_{xy}\right)^{(n)} z \mathrm{d}z \\
\left(P_x, P_y, P_{xy}\right) &= \sum_{n=1}^{3} \int_{h_{n-1}}^{h_n} \left(s_x,\ s_y,\ s_{xy}\right)^{(n)} f(z) \mathrm{d}z \\
\left(Q_x, Q_y\right) &= \sum_{n=1}^{3} \int_{h_{n-1}}^{h_n} \left(s_{xz},\ s_{yz}\right)^{(n)} g(z) \mathrm{d}z.
\end{aligned} \tag{18}$$

Substituting Eq. (13) into Eq. (18) and integrating through the thickness of the plates, and then reordering these equations into matrix form, one gets

$$\begin{Bmatrix} \mathbf{N} \\ \mathbf{M} \\ \mathbf{P} \\ \mathbf{Q} \end{Bmatrix} = \begin{bmatrix} \mathbf{A} & \mathbf{B} & \mathbf{E} & \mathbf{0} \\ \mathbf{B} & \mathbf{D} & \mathbf{F} & \mathbf{0} \\ \mathbf{E} & \mathbf{F} & \mathbf{H} & \mathbf{0} \\ \mathbf{0} & \mathbf{0} & \mathbf{0} & \mathbf{As} \end{bmatrix} \begin{Bmatrix} \boldsymbol{\varepsilon}^0 \\ \boldsymbol{\varepsilon}^1 \\ \boldsymbol{\varepsilon}^2 \\ \boldsymbol{\gamma}^0 \end{Bmatrix}, \tag{19}$$

where

$$\mathbf{N} = \begin{Bmatrix} N_x \\ N_y \\ N_{xy} \end{Bmatrix},\ \mathbf{M} = \begin{Bmatrix} M_x \\ M_y \\ M_{xy} \end{Bmatrix},\ \mathbf{P} = \begin{Bmatrix} P_x \\ P_y \\ P_{xy} \end{Bmatrix},\ \mathbf{Q} = \begin{Bmatrix} Q_x \\ Q_y \end{Bmatrix} \tag{20}$$

$$\boldsymbol{\varepsilon}^0 = \begin{Bmatrix} \varepsilon_x^0 \\ \varepsilon_y^0 \\ \gamma_{xy}^0 \end{Bmatrix},\ \boldsymbol{\varepsilon}^1 = \begin{Bmatrix} \varepsilon_x^1 \\ \varepsilon_y^1 \\ \gamma_{xy}^1 \end{Bmatrix},\ \boldsymbol{\varepsilon}^2 = \begin{Bmatrix} \varepsilon_x^2 \\ \varepsilon_y^2 \\ \gamma_{xy}^2 \end{Bmatrix},\ \boldsymbol{\gamma}^0 = \begin{Bmatrix} \gamma_{xz}^0 \\ \gamma_{yz}^0 \end{Bmatrix}, \tag{21}$$

and the elements of **A**, **B**, **D**, **F**, **H**, **As** are calculated as follows:

$$\begin{aligned}
&\left(Y_0, Y_1, Y_2, Y_3, Y_4, Y_5\right) \\
&\quad = \sum_{n=1}^{3} \int_{h_{n-1}}^{h_n} \mu(z)\rho(z)\left(1,\ z,\ f(z),\ z^2,\ zf(z),\ f^2(z)\right) \mathrm{d}z,
\end{aligned} \tag{22}$$

$$\left(\mathbf{As}_{ij}\right) = \sum_{n=1}^{3} \int_{h_{n-1}}^{h_n} C_{ij}^{(n)} \left(g^2(z)\right) \mathrm{d}z. \tag{23}$$

In addition, $I_0, I_1, I_2, I_3, I_4, I_5$ and $Y_0, Y_1, Y_2, Y_3, Y_4, Y_5$ in Eq. (17) are computed as follows:

$$\left(I_0, I_1, I_2, I_3, I_4, I_5\right) = \sum_{n=1}^{3} \int_{h_{n-1}}^{h_n} \rho(z)\left(1,\ z,\ f(z),\ z^2,\ zf(z),\ f^2(z)\right) \mathrm{d}z \tag{24}$$

$$\begin{aligned}
&\left(Y_0, Y_1, Y_2, Y_3, Y_4, Y_5\right) \\
&\quad = \sum_{n=1}^{3} \int_{h_{n-1}}^{h_n} \mu(z)\rho(z)\left(1,\ z,\ f(z),\ z^2,\ zf(z),\ f^2(z)\right) \mathrm{d}z,
\end{aligned} \tag{25}$$

where $\rho(z)$ is the effective mass density and $\mu(z)$ is effective nonlocal parameter of the materials. It is obvious that when the nonlocal parameter μ is constant, one gets $Y_i = \mu I_i$. As a consequence, the governing equations of motion Eq. (17) become the conventional governing equations of motion of the nanoplates with the constant nonlocal parameter which is usually used by many researchers in the literature. In this study, the nonlocal parameter is a material-dependent property of the material, and this is a key point of the present algorithm to investigate the role of the spatial variation of the nonlocal parameter on the free vibration of the FGSW nanoplates. For the parametric study, the nonlocal parameter of the metal phase will be chosen as a reference value and the ratio between the nonlocal parameter of ceramic phase and the nonlocal parameter of metal phase, $\varsigma = \mu_c/\mu_m$, is introduced as a new parameter. In the case of the constant nonlocal parameter, this parameter is equal to unit $\varsigma = 1$.

2.5 Analytical solution

In this study, an FGSW nanoplate subjected to simply support at all edges is considered. The Navier's solution technique is employed to solve the equations of motion, the unknown displacement functions of the nanoplates are assumed as the following formulae:

$$\begin{aligned}
u(x,y,t) &= \sum_{\alpha=1}^{\infty}\sum_{\beta=1}^{\infty} U_{\alpha\beta}\, e^{i\omega t} \cos\eta_\alpha x \sin\vartheta_\beta y \\
v(x,y,t) &= \sum_{\alpha=1}^{\infty}\sum_{\beta=1}^{\infty} V_{\alpha\beta}\, e^{i\omega t} \sin\eta_\alpha x \cos\vartheta_\beta y \\
w(x,y,t) &= \sum_{\alpha=1}^{\infty}\sum_{\beta=1}^{\infty} W_{\alpha\beta}\, e^{i\omega t} \sin\eta_\alpha x \sin\vartheta_\beta y \\
\varphi_x(x,y,t) &= \sum_{\alpha=1}^{\infty}\sum_{\beta=1}^{\infty} \Psi_{\alpha\beta}\, e^{i\omega t} \cos\eta_\alpha x \sin\vartheta_\beta y \\
\varphi_y(x,y,t) &= \sum_{\alpha=1}^{\infty}\sum_{\beta=1}^{\infty} \Upsilon_{\alpha\beta}\, e^{i\omega t} \sin\eta_\alpha x \cos\vartheta_\beta y,
\end{aligned} \tag{26}$$

where $\eta_\alpha = \alpha\pi/a$ and $\vartheta_\beta = \beta\pi/b$.

Substituting Eq. (26) into Eq. (19) and then Eq. (17), one gets

$$\left(\begin{bmatrix} k_{11} & k_{12} & k_{13} & k_{14} & k_{15} \\ & k_{22} & k_{23} & k_{24} & k_{25} \\ & & k_{33} & k_{34} & k_{35} \\ & sys & & k_{44} & k_{45} \\ & & & & k_{55} \end{bmatrix} - \omega^2 \begin{bmatrix} m_{11} & m_{12} & m_{13} & m_{14} & m_{15} \\ & m_{22} & m_{23} & m_{24} & m_{25} \\ & & m_{33} & m_{34} & m_{35} \\ & sys & & m_{44} & m_{45} \\ & & & & m_{55} \end{bmatrix}\right) \begin{Bmatrix} U_{\alpha\beta} \\ V_{\alpha\beta} \\ W_{\alpha\beta} \\ \Psi_{\alpha\beta} \\ \Upsilon_{\alpha\beta} \end{Bmatrix} = \begin{Bmatrix} 0 \\ 0 \\ 0 \\ 0 \\ 0 \end{Bmatrix}, \tag{27}$$

where k_{ij}, m_{ij}, $i,j = \overline{1,5}$ are calculated by the following formulae:

$$\begin{aligned}
&k_{11} = A_{11}\eta^2 + A_{66}\vartheta^2,\ \ k_{12} = \left(A_{12} + A_{66}\right)\vartheta\eta,\ \ k_{13} = -B_{11}\eta^3 - \left(B_{12} + 2B_{66}\right)\vartheta^2\eta,\\
&k_{14} = E_{11}\eta^2 + E_{66}\vartheta^2,\ \ k_{15} = \vartheta\left(E_{12} + E_{66}\right)\eta,\ \ k_{22} = A_{22}\vartheta^2 + A_{66}\eta^2,\\
&k_{23} = -B_{22}\vartheta^3 - \left(B_{12} + 2B_{66}\right)\eta^2\vartheta,\ \ k_{24} = \vartheta\left(E_{12} + E_{66}\right)\eta,\\
&k_{25} = E_{22}\vartheta^2 + \eta^2 E_{66},\ \ k_{33} = D_{22}\vartheta^4 + 2\eta^2\left(D_{12} + 2D_{66}\right)\vartheta^2 + D_{11}\eta^4,\\
&k_{34} = -\eta\left(F_{12} + 2F_{66}\right)\vartheta^2 - F_{11}\eta^3,\ \ k_{35} = -F_{22}\vartheta^3 - \left(F_{12} + 2F_{66}\right)\eta^2\vartheta,\\
&k_{44} = H_{11}\eta^2 + H_{66}\vartheta^2 + \mathrm{As}_{55},\ k_{45} = \vartheta\left(H_{12} + H_{66}\right)\eta,\ \ k_{55} = H_{22}\vartheta^2 + H_{66}\eta^2 + \mathrm{As}_{44}.
\end{aligned} \tag{28}$$

$$\begin{aligned}
&m_{11} = \lambda Y_0 + I_0,\ \ m_{12} = 0,\ \ m_{13} = -\eta\left(\lambda Y_1 + I_1\right),\ \ m_{14} = \lambda Y_2 + I_2,\ \ m_{15} = 0,\\
&m_{22} = \lambda Y_0 + I_0,\ \ m_{23} = -\vartheta\left(\lambda Y_1 + I_1\right),\ \ m_{24} = 0,\ \ m_{25} = \lambda Y_2 + I_2,\\
&m_{33} = \lambda\left(\lambda Y_3 + Y_0 + I_3\right) + I_0,\ \ m_{34} = -\eta\left(\lambda Y_4 + I_4\right),\ \ m_{35} = -\vartheta\left(\lambda Y_4 + I_4\right),\\
&m_{44} = \lambda Y_5 + I_5,\ \ m_{45} = 0,\ \ m_{55} = \lambda Y_5 + I_5,\\
&\lambda = \eta^2 + \vartheta^2.
\end{aligned} \tag{29}$$

3 Numerical results and discussion

3.1 Verification study

It is obvious that there is no available work that has been done on the free vibration analysis of the FGSW nanoplates, especially the free vibration of the FGSW nanoplates with the spatial variation of the nonlocal parameter. Thus, in this section, the accuracy of the present algorithm is verified via some examples of the sandwich plates and FG nanoplates with a constant nonlocal parameter. In such cases, the nonlocal parameters of two individual materials are equal to each other, so $\varsigma = \mu_c/\mu_m = 1$.

3.1.1 Free vibration of the FGSW plates

The main object of this subsection is to compare the frequencies of the FGSW plates of type C undergoing free vibration with different schemes and power-law indexes. The FGSW plates are made of Al and Al_2O_3, and the plate is subjected to simply support at four edges. The dimensions of the plates are $a = b$, $h = a/10$. The non-dimensional frequencies of the plates are calculated by $\overline{\omega} = \omega(a^2/h)\sqrt{\rho_0/E_0}$ with $\rho_0 = 1$ kg/m^3, $E_0 = 1$ GPa. The comparison of non-dimensional fundamental frequencies of the FGSW plates is presented in Table 2. The numerical results using the new IHSDT are compared with those of Meiche et al. [58] using four variables hyperbolic shear deformation theory and Li et al. [65] using the three-dimensional linear theory of elasticity. It can be seen that the present results are in good agreement with the available results for all cases of scheme and power-law indices.

Table 3 gives the comparison between the first ten non-dimensional frequencies of the FGSW plates using proposed theory and those of Meiche et al. [58] using SSDT and HySDT. The comparison shows that the present numerical results are very closed to the published results. Therefore, it can be concluded that the new IHSDT is compatible in predicting the free vibration of FGSW plates.

3.1.2 Free vibration of single-layer FG nanoplates

Continuously, the free vibration of single-layer nanoplates with a constant nonlocal parameter is considered and compared in this subsection. First, a thin FG nanoplate

Table 2 The comparison of the non-dimensional fundamental frequencies of the FGSW plates

p	Theory	1-0-1	2-1-2	2-1-1	1-1-1	2-2-1	1-2-1
0	Meiche et al. [58]	1.82449	1.82449	1.82449	1.82449	1.82449	1.82449
	Li et al. [65]	–	–	–	–	–	–
	Present	1.82445	1.82445	1.82445	1.82445	1.82445	1.82445
0.5	Meiche et al. [58]	1.44419	1.48405	1.50636	1.51922	1.54714	1.57458
	Li et al. [65]	1.44614	1.48608	1.50841	1.52131	1.54926	1.57668
	Present	1.44424	1.48408	1.50640	1.51922	1.54715	1.57452
1	Meiche et al. [58]	1.24310	1.30004	1.33328	1.35331	1.39559	1.43940
	Li et al. [65]	1.24470	1.30181	1.33511	1.35523	1.39763	1.44137
	Present	1.24319	1.30011	1.33339	1.35333	1.39565	1.43934
5	Meiche et al. [58]	0.94574	0.98166	1.03033	1.04455	1.10875	1.17397
	Li et al. [65]	0.94476	0.98103	1.02942	1.04532	1.10983	1.17567
	Present	0.94597	0.98183	1.03058	1.04466	1.10897	1.17397
10	Meiche et al. [58]	0.92811	0.94275	0.99184	0.99536	1.06081	1.12311
	Li et al. [65]	0.92727	0.94078	0.98929	0.99523	1.06104	1.12466
	Present	0.92837	0.94296	0.99210	0.99550	1.06106	1.12314

Table 3 The comparison of the non-dimensional first ten frequencies of the FGSW plates

α	β	1-2-1			2–2-1		
		Meiche et al. [58] (SSDT)	Meiche et al. [58] (HySDT)	Present	Meiche et al. [58] (SSDT)	Meiche et al. [58] (HySDT)	Present
1	1	1.30244	1.30250	1.30246	1.26780	1.24375	1.24389
1	2	3.15686	3.15726	3.15704	3.07382	3.01698	3.01776
2	2	4.90849	4.90978	4.90926	4.78065	4.69456	4.69633
1	3	6.02622	6.02866	6.02787	5.87022	5.76658	5.76916
2	3	7.63601	7.64154	7.64028	7.44002	7.31319	7.31712
1	4	9.67121	9.68465	9.68264	9.42552	9.27437	9.28028
3	3	10.16193	10.17821	10.17600	9.90439	9.74847	9.75490
2	4	11.12321	11.14644	11.14380	10.84261	10.67885	10.68634
3	4	13.41755	13.46652	13.46271	13.08260	12.91005	12.92026
4	4	16.39820	16.50693	16.50131	15.99393	15.83764	15.85170

of SUS304/Si_3N_4 simply supported at all edges with $p = 5$, $a = 10$ (nm) and $h/a = 0.05$ is considered. These FG nanoplates can be achieved easily by setting scheme of FGSW nanoplates of type A as (0-1-0). The non-dimensional frequency of the plates is calculated via $\hat{\omega} = \omega h\sqrt{\rho_c/G_c}$ with $G_c = E_c/(2(1+\nu))$. Table 4 gives the non-dimensional first three frequencies of the thin FG plates of the proposed theory in comparison with those of Zare et al. [31] in two cases of square and rectangular nanoplates [the superscript numbers are used to denote the mode order (α, β) of the frequencies]. According to this table, the present results are in excellent agreement with the published data.

Second, the present results of non-dimensional fundamental frequencies of the Al/Al_2O_3 FG nanoplates are compared with the results of Sobhy [33] and Hoa et al. [35] to confirm the validity of the proposed theory. It is noticed that the material properties of the plates are calculated via a new power-law of $P(z) = P_m\left(P_c/P_m\right)^{V_c}$, $V_c = (z/h + 1/2)^p$. In

Table 4 The comparison of the non-dimensional fundamental frequencies of thin FG nanoplates

b/a	μ (nm^2)	Method	Mode 1	Mode 2	Mode 3
1	0	Zare et al. [31]	0.0114^{11}	0.0281^{12}	0.0281^{21}
		Present	0.0113^{11}	0.0279^{12}	0.0279^{21}
	1	Zare et al. [31]	0.0104^{11}	0.0230^{12}	0.0230^{21}
		Present	0.0104^{11}	0.0229^{12}	0.0229^{21}
	4	Zare et al. [31]	0.0085^{11}	0.0165^{12}	0.0165^{21}
		Present	0.0085^{11}	0.0162^{12}	0.0162^{21}
0.5	0	Zare et al. [31]	0.0281^{11}	0.0443^{21}	0.0704^{31}
		Present	0.0279^{11}	0.0441^{21}	0.0701^{31}
	1	Zare et al. [31]	0.0230^{11}	0.0330^{21}	0.0466^{31}
		Present	0.0229^{11}	0.0330^{21}	0.0464^{31}
	4	Zare et al. [31]	0.0165^{11}	0.0218^{21}	0.0286^{31}
		Present	0.0162^{11}	0.0216^{21}	0.0283^{31}

which, the results of Sobhy [33] are obtained via two-variable shear deformation theory and the results of Hoa et al. [35] are calculated via single variable shear deformation theory. The dimensions of the plates are $a = b = 10$ (nm), $h/a = 0.1$. The comparison is given in Table 5, in which the non-dimensional fundamental frequencies are computed by $\tilde{\omega} = \omega(a^2/\pi^2)\sqrt{\rho_c h/D_c}$, $D_c = E_c h^3/(12(1-\nu^2))$. The comparison shows that the difference between the present results and those of Sobhy [33] and Hoa et al. [35] is very low. Hence, the proposed theory is compatible to examine the free vibration of nanoplates.Kindly provide the significance for the bold values mentioned in Tables 2, 3, 4, 5The bold style in these Tables is used to help reviewer read the manuscript more easily, it is unnecessary in the final artical. So please can you change the bole values to normal values.

According to the above comparison studies, it can be concluded that the proposed algorithm is good accuracy and compatible to predict the behavior of the FGSW nanoplates undergoing free vibration.

3.2 Parametric study

In this section, a comprehensive study on the role of the spatial variation of the nonlocal parameters on the free vibration of the Al/Al_2O_3 FGSW nanoplates is presented. The dimensions of the FGSW nanoplates are $a \times b$, the total height is h, and the boundary conditions of the plates are simply supported at all edges. It is noticed that, in the parameter study section, the nonlocal parameter of the metal phase, $\mu_m = 2$ (nm^2), is chosen as the reference value and that of the ceramic phase is calculated via ratio $\varsigma = \mu_c/\mu_m$. For convenience, the following dimensionless frequency is used:

$$\omega^* = \omega \frac{a^2}{h_0}\sqrt{\frac{\rho_0}{E_0}}, \tag{30}$$

where $E_0 = 1$ GPa, $\rho_0 = 1$ kg/m^3, $h_0 = a/10$.

The non-dimensional fundamental frequencies of square FGSW nanoplates of Al/Al_2O_3 with $b = a = 10$ (nm), $a/h = 10$ are demonstrated in Table 6. In addition, the non-dimensional first six frequencies of the FGSW nanoplates with $b = a = 10$ (nm), $a/h = 10$, $p = 2$ are given in Table 7.

Next, the effects of the aspect ratio on the behavior of (1-2-1) FGSW nanoplates of Al/Al_2O_3 with $b = a = 10$ (nm) undergoing free vibration are investigated. The side-to-thickness ratio of the plate is $a/h = 10$, the power-law index is $p = 2$, the aspect ratio b/a changes from 0.5 to 5, and the ratios of the nonlocal parameters are $\varsigma = 0.5,\ 1,\ 1.5,\ 2$. The non-dimensional fundamental frequencies of the FGSW nanoplates as the function of the aspect ratio b/a with four cases of the nonlocal parameter's ratio are plotted in Fig. 3. It can see clearly that the non-dimensional frequencies of the FGSW nanoplates decrease rapidly as increasing of the aspect ratio b/a. The fundamental frequencies decrease dramatically when the aspect ratio varies from 0.5 to 2, then the fundamental frequencies decrease slowly. According to the four subplots of Fig. 3, the frequencies of the FGSW nanoplates with a small value of the nonlocal parameter's ratio are higher than those of the FGSW nanoplates with higher nonlocal parameter's ratio. The frequencies of the FGSW nanoplates of type A is similar to those of type B, and the frequencies of the FGSW nanoplates of type C are higher than those of type A and type B.

Figure 4 presents the influence of the side-to-thickness ratio a/h on the fundamental frequencies of the square (1-2-1) FGSW nanoplates of Al/Al_2O_3 with $a = b = 10$ (nm). The power-law index of the materials is $p = 2$, and four cases of the nonlocal parameters are $\varsigma = 0.5,\ 1,\ 1.5,\ 2$. According to this figure, it is obvious that the side-to-thickness ratio has remarkable effects on the free vibration behavior of the FGSW nanoplates. When the side-to-thickness ratio rises, the non-dimensional fundamental frequencies of the FGSW nanoplates decrease. The reason is that when the side-to-thickness ratio increases, the FGSW nanoplates become thin plates, so the stiffness of the plates is reduced. It can be seen against that the fundamental frequencies of the FGSW nanoplates of type C are higher than those of type B, and the fundamental frequencies of the FGSW nanoplates of type A are smallest. Because the FGSW nanoplates of type C consist of two FG face sheets with the ceramic-rich surface at the top and bottom surface of the FGSW nanoplates, so the stiffness of the FGSW nanoplates of type C greater than those of type B which consist of two FG face sheets with the metal-rich surface at the top and bottom surface of the plates. The non-dimensional fundamental frequencies of the

Table 5 The comparison of the non-dimensional fundamental frequencies of the FG nanoplates

p	$\mu = 0$			$\mu = 4$		
	Sobhy [33]	Hoa et al. [35]	Present	Sobhy [33]	Hoa et al. [35]	Present
0	1.9318	1.9317	1.9317	1.4441	1.4440	1.4440
0.5	1.4969	1.4989	1.4968	1.1189	1.1205	1.1189
2.5	1.2572	1.2623	1.2574	0.9397	0.9436	0.9399
5.5	1.2087	1.2126	1.2088	0.9035	0.9065	0.9036
10.5	1.1609	1.1618	1.1609	0.8678	0.8685	0.8678

Table 6 The non-dimensional fundamental frequencies of the square FGSW nanoplates ($a/h = 10$)

Types	p	ς	1-0-1	2-1-2	2-1-1	1-1-1	2-2-1	1-2-1
Type A	0	0.5	1.08522	1.13716	1.08522	1.19155	1.13716	1.28128
		1	1.04001	1.08183	1.04001	1.12823	1.08183	1.20628
		1.5	1.00003	1.03386	1.00003	1.07405	1.03386	1.14307
		2	0.96432	0.99176	0.96432	1.02699	0.99176	1.08887
	2	0.5	1.08522	1.07917	1.06299	1.08108	1.06680	1.08776
		1	1.04001	1.03752	1.03287	1.04158	1.03709	1.05084
		1.5	1.00003	1.00035	1.00517	1.00612	1.00973	1.01745
		2	0.96432	0.96691	0.97958	0.97405	0.98443	0.98704
Type B	0	0.5	1.66730	1.66730	1.66730	1.66730	1.66730	1.66730
		1	1.54482	1.54482	1.54482	1.54482	1.54482	1.54482
		1.5	1.44590	1.44590	1.44590	1.44590	1.44590	1.44590
		2	1.36382	1.36382	1.36382	1.36382	1.36382	1.36382
	2	0.5	0.92265	0.98666	1.02709	1.05215	1.10504	1.16293
		1	0.89875	0.95037	0.98665	1.00628	1.05324	1.10283
		1.5	0.87662	0.91781	0.95064	0.96593	1.00810	1.05119
		2	0.85604	0.88838	0.91831	0.93008	0.96831	1.00618
Type C	0	0.5	0.78557	0.78557	0.78557	0.78557	0.78557	0.78557
		1	0.78557	0.78557	0.78557	0.78557	0.78557	0.78557
		1.5	0.78557	0.78557	0.78557	0.78557	0.78557	0.78557
		2	0.78557	0.78557	0.78557	0.78557	0.78557	0.78557
	2	0.5	1.61636	1.57902	1.53028	1.53555	1.47334	1.45470
		1	1.53444	1.51228	1.46909	1.47989	1.42466	1.41363
		1.5	1.46384	1.45335	1.41471	1.42987	1.38050	1.37586
		2	1.40216	1.40081	1.36595	1.38460	1.34021	1.34096

FGSW nanoplates with a higher ratio of nonlocal parameters are smaller than those of the FGSW nanoplates with a small value of nonlocal parameter's ratio.

Continuously, the dependence of the fundamental frequencies of the square (1-2-1) FGSW nanoplates of Al/Al_2O_3 with $a = b = 10$ (nm) on the power-law index is investigated in details. The side-to-thickness of the plates is $a/h = 10$, and four cases of the nonlocal parameters' ratio are considered, which are $\varsigma = 0.5,\ 1,\ 1.5,\ 2$. Figure 5 demonstrates the variation of the fundamental frequencies of the FGSW nanoplates as the function of the power-law index. When the power-law index increases, the fundamental frequencies of the FGSW nanoplates of type A and type B decrease, while those of the FGSW nanoplates of type C increase in four cases of the ratio of the nonlocal parameters. The fundamental frequencies of the FGSW nanoplates of type B decrease faster than those of the FGSW nanoplates of type A. It is because when the power-law index increases, the volume fraction of the ceramic component of type A and type B decreases and the metallic component increases, so the stiffness of the FGSW nanoplates of type A and type B decrease. On the other hand, when the power-law index increases, the volume fraction of the ceramic component of type C increase and the metallic component decrease, it leads to reduce the stiffness of the FGSW nanoplates. In addition, the consideration of the higher value of the nonlocal parameter's ratio leads to a reduction of the fundamental frequencies of the FGSW nanoplates.

Finally, the effects of the variation of the nonlocal parameter on the free vibration of the FGSW nanoplates are considered judiciously. An Al/Al_2O_3 (1–2-1) FGSW nanoplates with side-to-thickness of $a/h = 5,\ 10$ and the power-law index of $p = 0.5,\ 2$ is examined herein. The ratio of the nonlocal parameters varies from 0.5 to 2. Figure 6 demonstrates the influence of the nonlocal parameter's ratio on the fundamental frequencies of the FGSW nanoplates. It can be seen that when the ratio of the nonlocal parameters rises, the fundamental frequencies of the FGSW nanoplates of three cases of type A, type B, and type C decrease. In the case of $p = 0.5$, the decrease rate of the frequency of the FGSW nanoplates of type B is highest and that of the FGSW nanoplates of type C is lowest. In the case of $p = 2$, the decrease rates of the frequencies of the FGSW nanoplates of type A and C are similar and lower than those of the FGSW nanoplates of type B.

Figure 7 shows the ratio between the frequencies of the rectangular FGSW nanoplates with variable nonlocal parameter and those of the nanoplates with a constant nonlocal parameter of $\mu_c = \mu_m = 2$. In which the dimensions of the plates are $a = 10$ (nm), $b = 20$ (nm). According to

Table 7 The non-dimensional first six frequencies of the square FGSW nanoplates ($p = 2$)

Types	Scheme	ς	Mode 1	Mode 2	Mode 3	Mode 4	Mode 5	Mode 6
Type A	1-1-1	0.5	1.08108	2.24115	2.24115	3.08570	3.53858	3.53858
		1	1.04158	2.09782	2.09782	2.84392	3.23933	3.23933
		1.5	1.00612	1.97887	1.97887	2.65123	3.00492	3.00492
		2	0.97405	1.87809	1.87809	2.49300	2.81491	2.81491
	1-2-1	0.5	1.08776	2.24533	2.24533	3.08243	3.52947	3.52947
		1	1.05084	2.11195	2.11195	2.85801	3.25204	3.25204
		1.5	1.01745	1.99981	1.99981	2.67632	3.03103	3.03103
		2	0.98704	1.90382	1.90382	2.52535	2.84963	2.84963
	2-2-1	0.5	1.06680	2.17743	2.17743	2.96607	3.38249	3.38249
		1	1.03709	2.07161	2.07161	2.78959	3.16525	3.16525
		1.5	1.00973	1.97983	1.97983	2.64120	2.98499	2.98499
		2	0.98443	1.89926	1.89926	2.51417	2.83231	2.83231
Type B	1-1-1	0.5	1.05215	2.21983	2.21983	3.09672	3.57669	3.57669
		1	1.00628	2.04893	2.04893	2.80289	3.20935	3.20935
		1.5	0.96593	1.91227	1.91227	2.57943	2.93601	2.93601
		2	0.93008	1.79974	1.79974	2.40209	2.72239	2.72239
	1-2-1	0.5	1.16293	2.46603	2.46603	3.44866	3.98677	3.98677
		1	1.10283	2.23968	2.23968	3.05688	3.49542	3.49542
		1.5	1.05119	2.06604	2.06604	2.77405	3.15004	3.15004
		2	1.00618	1.92739	1.92739	2.55753	2.89023	2.89023
	2-2-1	0.5	1.10504	2.33454	2.33454	3.25793	3.76284	3.76284
		1	1.05324	2.14087	2.14087	2.92430	3.34540	3.34540
		1.5	1.00810	1.98857	1.98857	2.67583	3.04179	3.04179
		2	0.96831	1.86474	1.86474	2.48154	2.80820	2.80820
Type C	1-1-1	0.5	1.53555	3.04428	3.04428	4.05148	4.55963	4.55963
		1	1.47989	2.84623	2.84623	3.72248	4.15601	4.15601
		1.5	1.42987	2.68240	2.68240	3.46248	3.84351	3.84351
		2	1.38460	2.54395	2.54395	3.25030	3.59232	3.59232
	1-2-1	0.5	1.45470	2.84112	2.84112	3.74415	4.19305	4.19305
		1	1.41363	2.69740	2.69740	3.50802	3.90497	3.90497
		1.5	1.37586	2.57349	2.57349	3.31157	3.66911	3.66911
		2	1.34096	2.46522	2.46522	3.14480	3.47138	3.47138
	2-2-1	0.5	1.47334	2.92542	2.92542	3.89934	4.39267	4.39267
		1	1.42466	2.75225	2.75225	3.61143	4.03917	4.03917
		1.5	1.38050	2.60658	2.60658	3.37911	3.75922	3.75922
		2	1.34021	2.48183	2.48183	3.18652	3.53040	3.53040

this figure, it is obvious that the variation of the nonlocal parameter has significant effects on the higher frequencies of the FG nanoplates and the FGSW nanoplates. When the ratio of the nonlocal parameters increases, the higher frequencies decreases faster than the lower ones of the FGSW nanoplates. Hence, it can be concluded that it is necessary to take into account the effects of the variation of the nonlocal parameters in designing, testing, and producing inhomogeneous nanostructures.

4 Conclusions

In this work, the role of the spatial variation of the nonlocal parameter on the free vibration of the FGSW nanoplates has been investigated for the first time. Moreover, a new inverse hyperbolic shear deformation theory in combination with modified nonlocal elasticity theory has been established to take into account the spatial variation of the nonlocal parameter. A comprehensive study on the effects of several parameters including the variation of the nonlocal parameter, the power-law index, the aspect ratio, as well as the side-to-thickness ratio has been carried out.

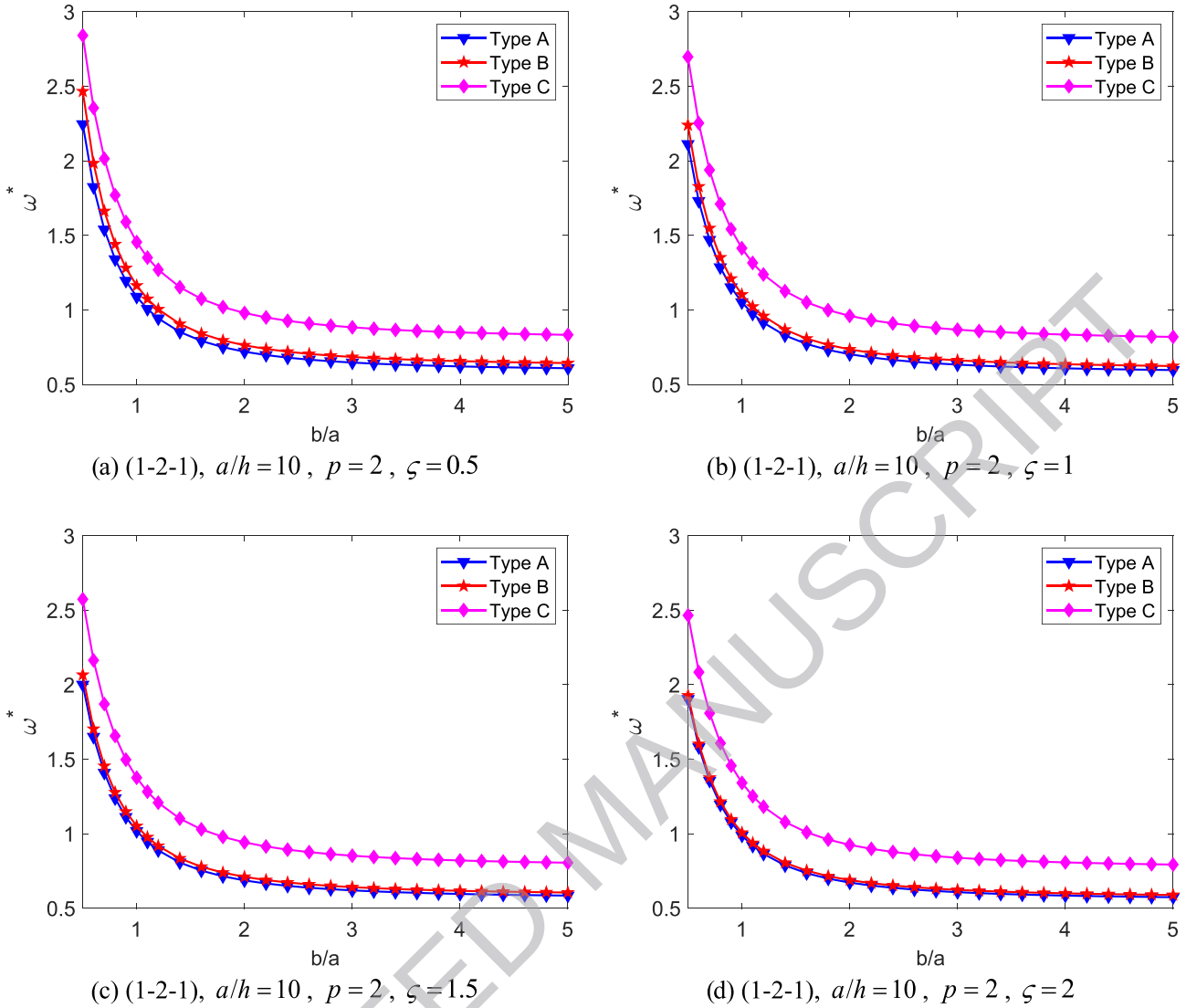

Fig. 3 The effects of aspect ratio b/a on the fundamental frequencies of the FGSW nanoplates

The numerical results of this work drew some remarkable points as follows.

- The spatial variation of the nonlocal parameter plays a significant role in the behavior of the FGSW nanoplates undergoing free vibrations.
- The consideration of the nonlocal parameter leads to a reduction of the natural frequencies of the FGSW nanoplates.
- The variation of the nonlocal parameter has significant effects on the higher frequencies of the FGSW nanoplates.
- Because the nonlocal parameter is a material-dependent property, more investigations on the role of the spatial variation of the nonlocal parameter on static bending, free vibration, buckling, as well as dynamic response of the FG and FGSW nanoplates, nanobeams should be done to understanding deeply the mechanical behavior of the nanostructures. Furthermore, the vibration of the FGSW nanoplates can be controlled by varying the material volume fractions to avoid resonant phenomenon in micro/nanoelectromechanical systems. Besides, the measurement of the exact nonlocal parameter of FGMs of the nanostructures is the challenge of the future works.

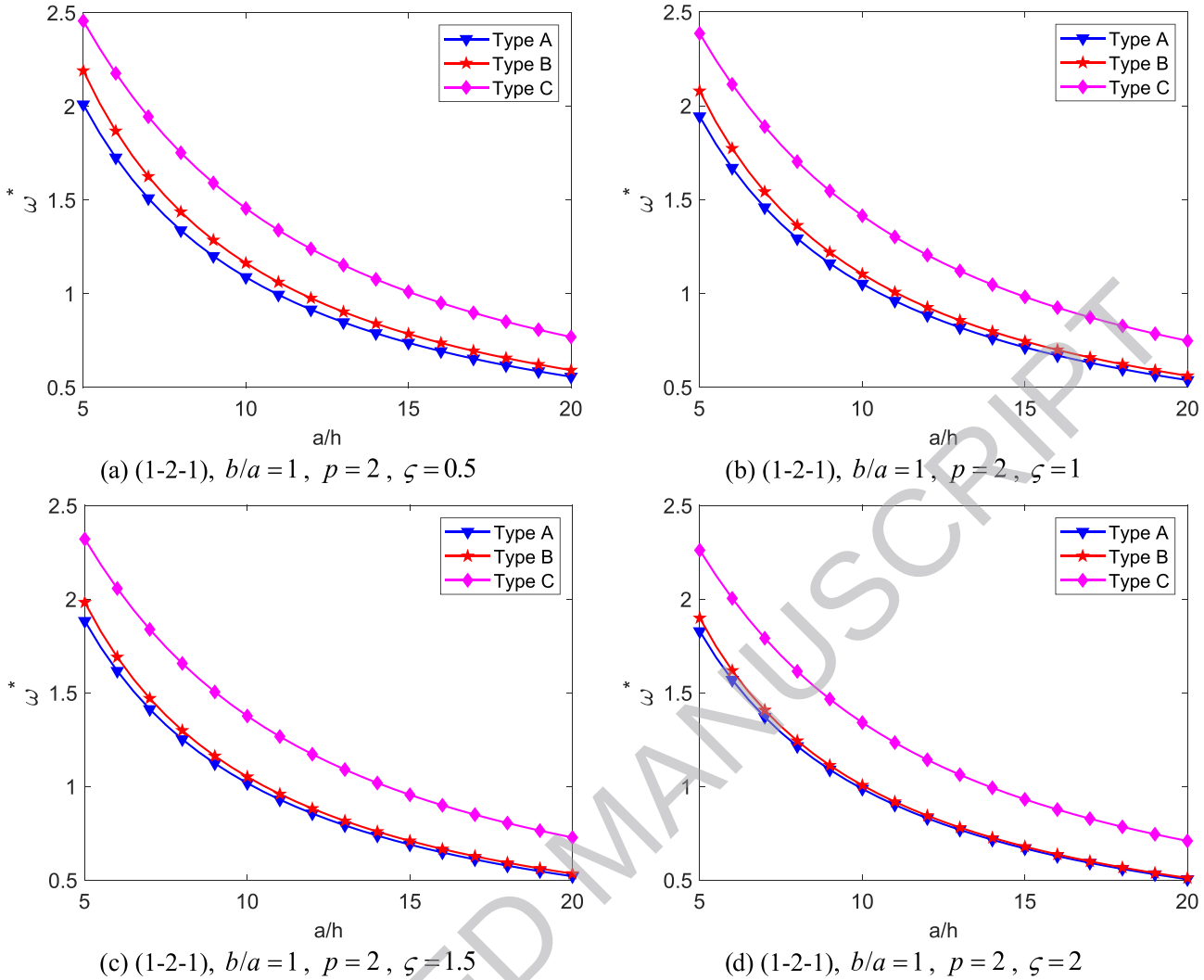

(a) (1-2-1), $b/a=1$, $p=2$, $\varsigma=0.5$

(b) (1-2-1), $b/a=1$, $p=2$, $\varsigma=1$

(c) (1-2-1), $b/a=1$, $p=2$, $\varsigma=1.5$

(d) (1-2-1), $b/a=1$, $p=2$, $\varsigma=2$

Fig. 4 The influence of the side-to-thickness ratio a/h on the fundamental frequencies of the FGSW nanoplates

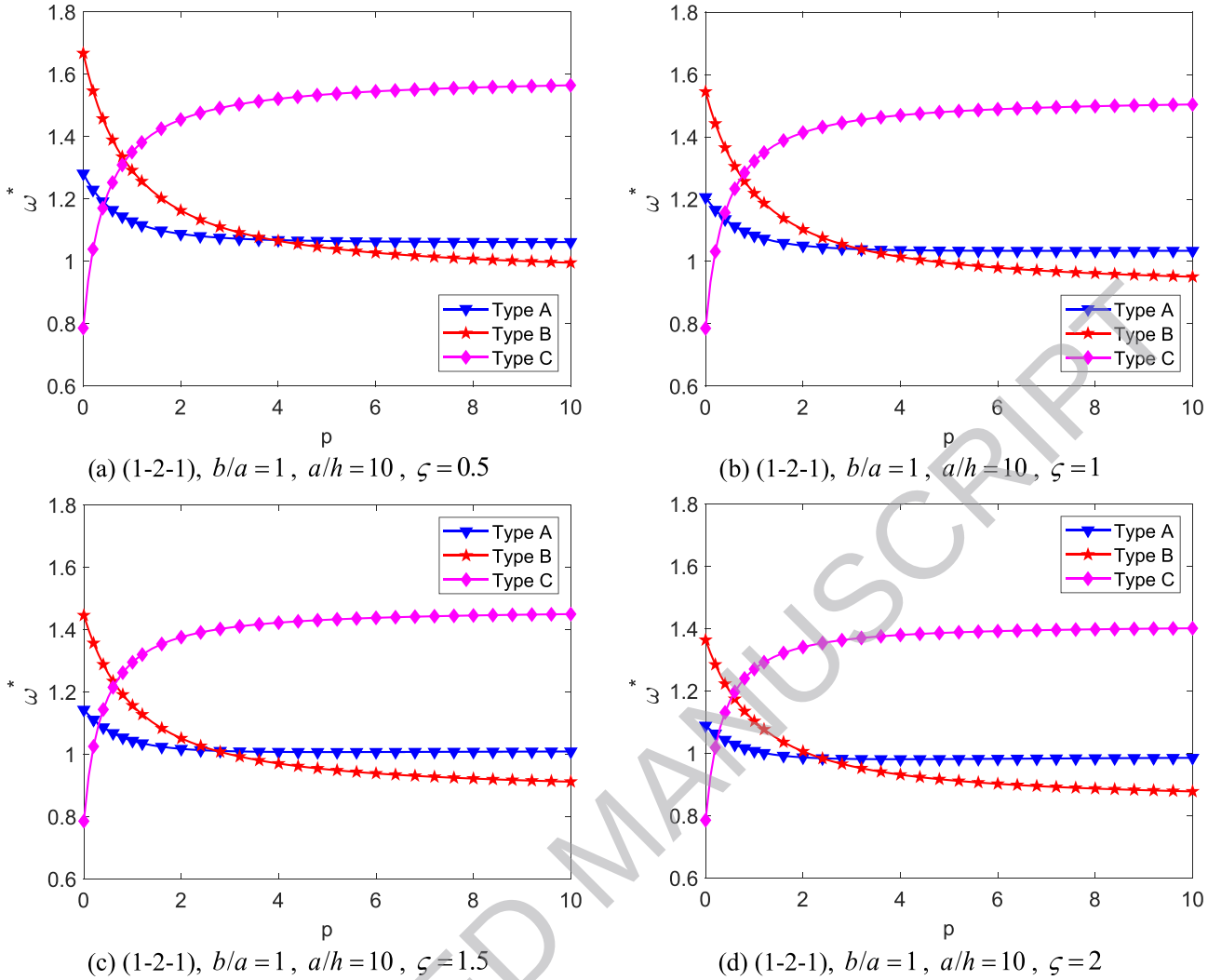

(a) (1-2-1), $b/a=1$, $a/h=10$, $\varsigma=0.5$

(b) (1-2-1), $b/a=1$, $a/h=10$, $\varsigma=1$

(c) (1-2-1), $b/a=1$, $a/h=10$, $\varsigma=1.5$

(d) (1-2-1), $b/a=1$, $a/h=10$, $\varsigma=2$

Fig. 5 The variation of the fundamental frequencies of the FGSW nanoplates as function of the power-law index p

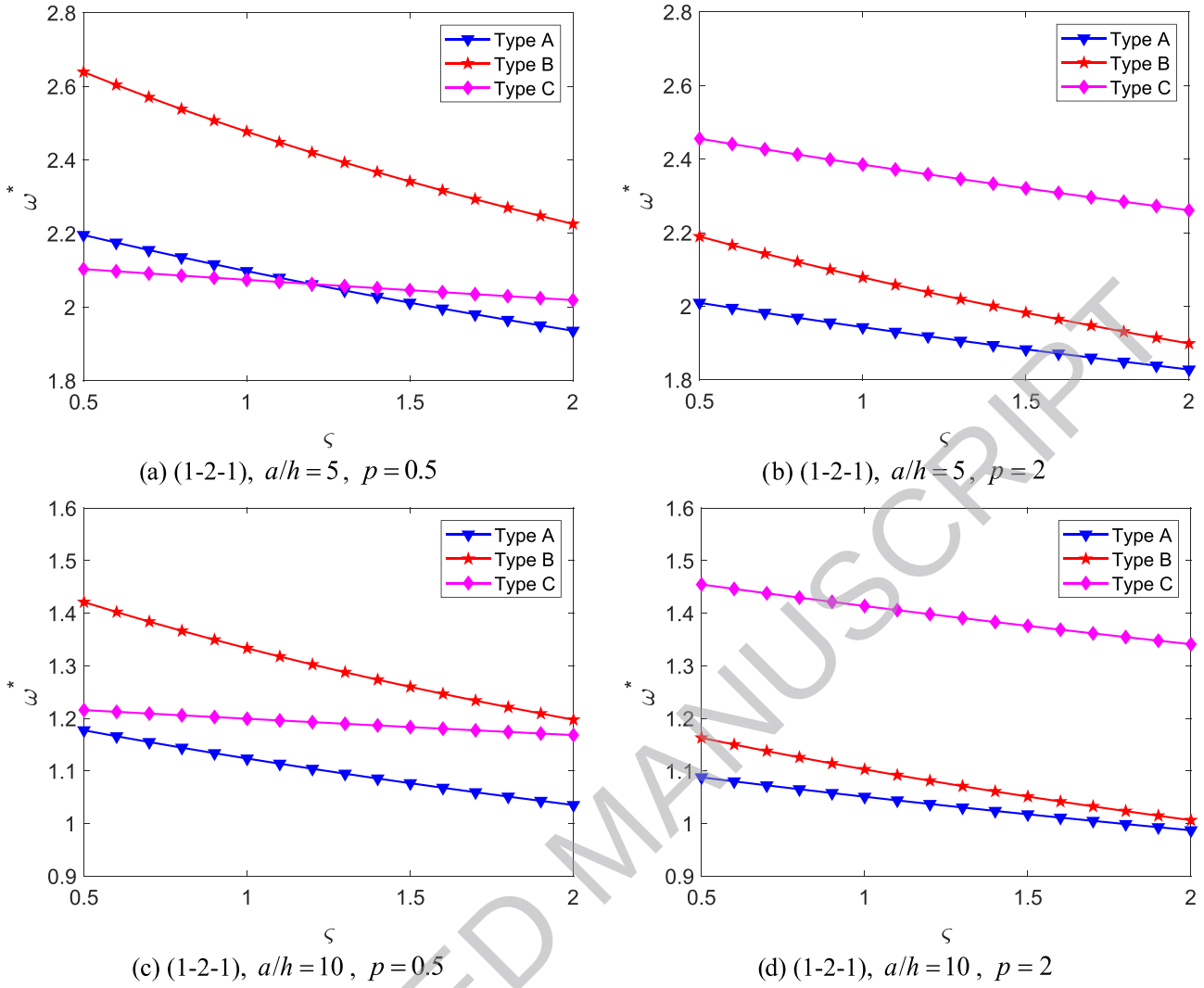

Fig. 6 The effects of the ratio of nonlocal parameters ς on the fundamental frequencies of the FGSW nanoplates

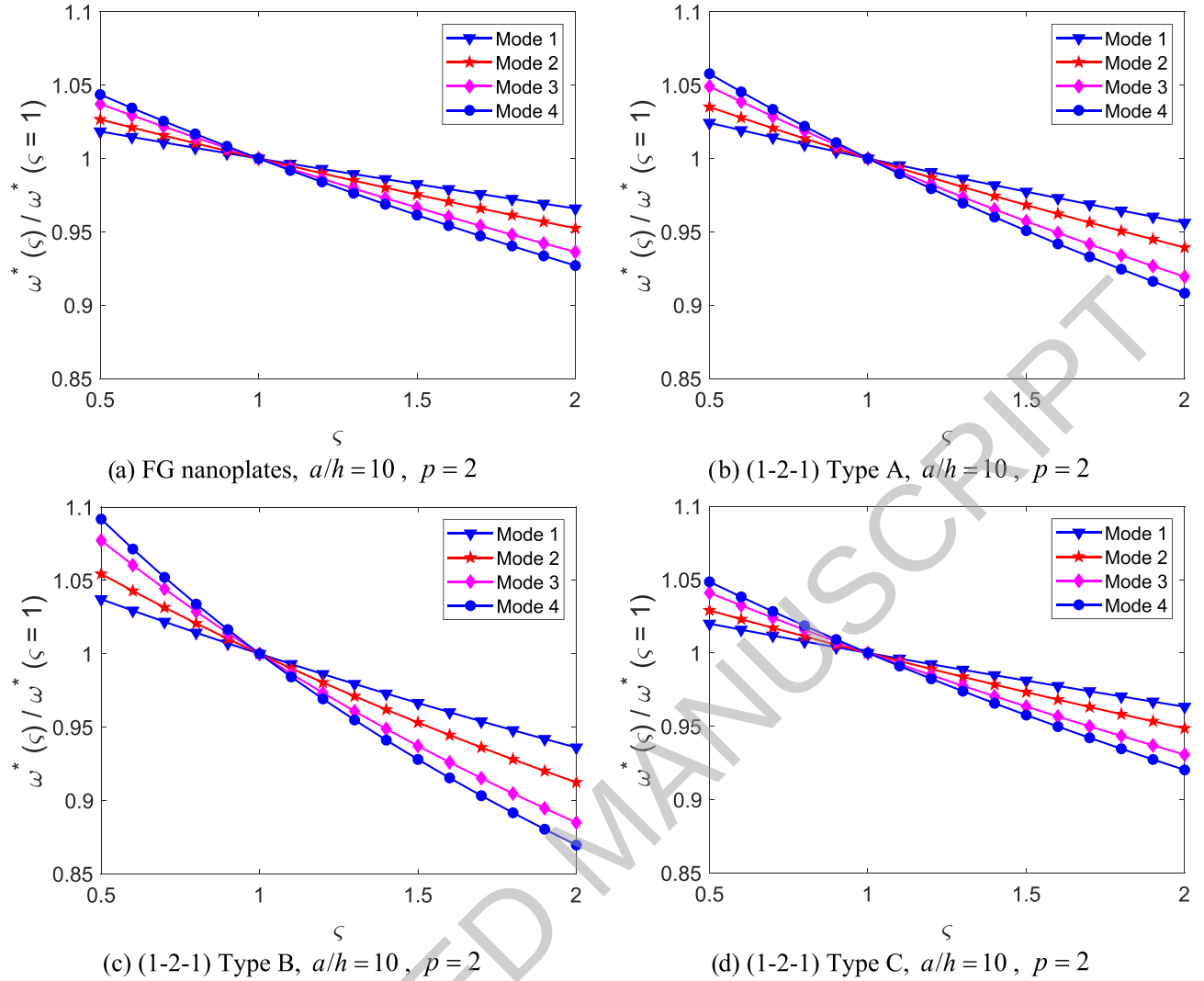

Fig. 7 The ratio of the frequencies of the FGSW nanoplates as function of ς

Funding This research received no specific grant from any funding agency in the public, commercial, or not-for-profit sectors.

Declarations

Conflict of interests The author(s) declares that there is no conflict of interest.

References

1. Yang F, Chong ACM, Lam DCC, Tong P (2002) Couple stress based strain gradient theory for elasticity. Int J Solids Struct 39(10):2731–2743. https://doi.org/10.1016/S0020-7683(02)00152-X
2. Arefi M, Firouzeh S, Bidgoli EMR, Civalek O (2022) Analysis of porous micro-plates reinforced with FG-GNPs based on Reddy plate theory. Compos Struct 247:112391. https://doi.org/10.1016/j.compstruct.2020.112391
3. Gurtin ME, Markenscoff X, Thurston RN (1976) Effect of surface stress on the natural frequency of thin crystals. Appl Phys Lett 29(9):529–530. https://doi.org/10.1063/1.89173
4. Guo J-G, Zhao Y-P (2007) The size-dependent bending elastic properties of nanobeams with surface effects. Nanotechnology 18(29):295701. https://doi.org/10.1088/0957-4484/18/29/295701
5. Abo-Bakr RM, Eltaher MA, Attia MA (2020) Pull-in and free-standing instability of actuated functionally graded nanobeams including surface and stiffening effects. Eng Comput. https://doi.org/10.1007/s00366-020-01146-0
6. Abdelrahman AA, Eltaher MA (2020) On bending and buckling responses of perforated nanobeams including surface energy for different beams theories. Eng Comput. https://doi.org/10.1007/s00366-020-01211-8
7. Farshi B, Assadi A, Alinia-ziazi A (2010) Frequency analysis of nanotubes with consideration of surface effects. Appl Phys Lett 96(9):93105. https://doi.org/10.1063/1.3332579

8. Lu P, He LH, Lee HP, Lu C (2006) Thin plate theory including surface effects. Int J Solids Struct 43(16):4631–4647. https://doi.org/10.1016/j.ijsolstr.2005.07.036
9. Fleck NA, Muller GM, Ashby MF, Hutchinson JW (1994) Strain gradient plasticity: Theory and experiment. Acta Metall Mater 42(2):475–487. https://doi.org/10.1016/0956-7151(94)90502-9
10. Aifantis EC (1999) Strain gradient interpretation of size effects. Int J Fract 95(1):299. https://doi.org/10.1023/A:1018625006804
11. Phung-Van P, Chien CH (2021) A novel size-dependent nonlocal strain gradient isogeometric model for functionally graded carbon nanotube-reinforced composite nanoplates. Eng Comput. https://doi.org/10.1007/s00366-021-01353-3
12. Esen I, Abdelrhmaan AA, Eltaher MA (2021) Free vibration and buckling stability of FG nanobeams exposed to magnetic and thermal fields. Eng Comput. https://doi.org/10.1007/s00366-021-01389-5
13. Eringen AC (1967) Theory of micropolar plates. Zeitschrift für Angew Math und Phys ZAMP 18(1):12–30. https://doi.org/10.1007/BF01593891
14. Eringen AC (1972) Nonlocal polar elastic continua. Int J Eng Sci 10(1):1–16. https://doi.org/10.1016/0020-7225(72)90070-5
15. Eringen AC, Edelen DGB (1972) On nonlocal elasticity. Int J Eng Sci 10(3):233–248. https://doi.org/10.1016/0020-7225(72)90039-0
16. Eringen AC (1983) On differential equations of nonlocal elasticity and solutions of screw dislocation and surface waves. J Appl Phys 54(9):4703–4710. https://doi.org/10.1063/1.332803
17. Reddy JN (2007) Nonlocal theories for bending, buckling and vibration of beams. Int J Eng Sci 45(2):288–307. https://doi.org/10.1016/j.ijengsci.2007.04.004
18. Reddy JN, Pang SD (2008) Nonlocal continuum theories of beams for the analysis of carbon nanotubes. J Appl Phys 103(2):23511. https://doi.org/10.1063/1.2833431
19. Ebrahimi F, Barati MR, Zenkour AM (2017) Vibration analysis of smart embedded shear deformable nonhomogeneous piezoelectric nanoscale beams based on nonlocal elasticity theory. Int J Aeronaut Sp Sci 18(2):255–269. https://doi.org/10.5139/IJASS.2017.18.2.255
20. Thai H-T, Vo TP (2012) A nonlocal sinusoidal shear deformation beam theory with application to bending, buckling, and vibration of nanobeams. Int J Eng Sci 54:58–66. https://doi.org/10.1016/j.ijengsci.2012.01.009
21. Eltaher MA, Emam SA, Mahmoud FF (2012) Free vibration analysis of functionally graded size-dependent nanobeams. Appl Math Comput 218(14):7406–7420. https://doi.org/10.1016/j.amc.2011.12.090
22. Nazemnezhad R, Hosseini-Hashemi S (2014) Nonlocal nonlinear free vibration of functionally graded nanobeams. Compos Struct 110:192–199. https://doi.org/10.1016/j.compstruct.2013.12.006
23. Ebrahimi F, Barati MR, Civalek O (2020) Application of Chebyshev-Ritz method for static stability and vibration analysis of nonlocal microstructure-dependent nanostructures. Eng Comput 36:953–964. https://doi.org/10.1007/s00366-019-00742-z
24. Hadji L, Avcar M (2021) Nonlocal free vibration analysis of porous FG nanobeams using hyperbolic shear deformation beam theory. Adv Nano Res 10(3):281–293. https://doi.org/10.12989/anr.2021.10.3.281
25. Youcef G, Ahmed H, Abdelillah B, Mohamed Z (2020) Porosity-dependent free vibration analysis of FG nanobeam using non-local shear deformation and energy principle. Adv Nano Res 8(1):37–47. https://doi.org/10.12989/anr.2020.8.1.037
26. Shariati A, Jung DW, Sedighi HM, Zur KK, Habibi M, Safa M (2020) "On the vibrations and stability of moving viscoelastic axially functionally graded nanobeams. Materials 13(7):1707. https://doi.org/10.3390/ma13071707
27. Zenkour AM (2018) A novel mixed nonlocal elasticity theory for thermoelastic vibration of nanoplates. Compos Struct 185:821–833. https://doi.org/10.1016/j.compstruct.2017.10.085
28. Aghababaei R, Reddy JN (2009) Nonlocal third-order shear deformation plate theory with application to bending and vibration of plates. J Sound Vib 326(1):277–289. https://doi.org/10.1016/j.jsv.2009.04.044
29. Aksencer T, Aydogdu M (2011) Levy type solution method for vibration and buckling of nanoplates using nonlocal elasticity theory. Phys E Low-dimens Syst Nanostruct 43(4):954–959. https://doi.org/10.1016/j.physe.2010.11.024
30. Hosseini-Hashemi S, Bedroud M, Nazemnezhad R (2013) An exact analytical solution for free vibration of functionally graded circular/annular Mindlin nanoplates via nonlocal elasticity. Compos Struct 103:108–118. https://doi.org/10.1016/j.compstruct.2013.02.022
31. Zare M, Nazemnezhad R, Hosseini-Hashemi S (2015) Natural frequency analysis of functionally graded rectangular nanoplates with different boundary conditions via an analytical method. Meccanica 50(9):2391–2408. https://doi.org/10.1007/s11012-015-0161-9
32. Sobhy M (2014) Natural frequency and buckling of orthotropic nanoplates resting on two-parameter elastic foundations with various boundary conditions. J Mech 30(5):443–453. https://doi.org/10.1017/jmech.2014.46
33. Sobhy M (2015) A comprehensive study on FGM nanoplates embedded in an elastic medium. Compos Struct 134:966–980. https://doi.org/10.1016/j.compstruct.2015.08.102
34. Sobhy M, Radwan AF (2017) A new quasi 3D nonlocal plate theory for vibration and buckling of FGM nanoplates. Int J Appl Mech 09(01):1750008. https://doi.org/10.1142/S1758825117500089
35. Hoa LK, Vinh PV, Duc ND, Trung NT, Son LT, Thom DV (2020) "Bending and free vibration analyses of functionally graded material nanoplates via a novel nonlocal single variable shear deformation plate theory. Proc Inst Mech Eng Part C J Mech Eng Sci 15:14. https://doi.org/10.1177/0954406220964522
36. Akbas SD (2020) Modal analysis of viscoelastic nanorods under an axially harmonic load. Adv Nano Res 8(4):277–282. https://doi.org/10.12989/anr.2020.8.4.277
37. Ghandourah EE, Abdraboh AM (2020) Dynamic analysis of functionally graded nonlocal nanobeam with different porosity models. Steel Compos Struct 36(3):293–305. https://doi.org/10.12989/scs.2020.36.3.293
38. Natarajan S, Chakraborty S, Thangavel M, Bordas S, Rabczuk T (2012) Size-dependent free flexural vibration behavior of functionally graded nanoplates. Comput Mater Sci 65:74–80. https://doi.org/10.1016/j.commatsci.2012.06.031
39. Koizumi M (1997) FGM activities in Japan. Compos Part B Eng 28(1):1–4. https://doi.org/10.1016/S1359-8368(96)00016-9
40. Swaminathan K, Naveenkumar DT, Zenkour AM, Carrera E (2015) Stress, vibration and buckling analyses of FGM plates—a state-of-the-art review. Compos Struct 120:10–31. https://doi.org/10.1016/j.compstruct.2014.09.070
41. Sayyad AS, Ghugal YM (2019) Modeling and analysis of functionally graded sandwich beams: a review. Mech Adv Mater Struct 26(21):1776–1795. https://doi.org/10.1080/15376494.2018.1447178
42. Thom DV, Vinh PV, Nam NH (2020) On the development of refined plate theory for static bending behavior of functionally graded plates. Math Probl Eng. https://doi.org/10.1155/2020/2836763
43. Vinh PV, Dung NT, Tho NC, Thom DV, Hoa LK (2021) Modified single variable shear deformation plate theory for free vibration

analysis of rectangular FGM plates. Structures 29:1435–1444. https://doi.org/10.1016/j.istruc.2020.12.027
44. Abouelregal AE, Mohammed WW, Mohammad-Sedighi H (2021) Vibration analysis of functionally graded microbeam under initial stress via a generalized thermoelastic model with dual-phase lags. Arch Appl Mech 91(5):2127–2142. https://doi.org/10.1007/s00419-020-01873-2
45. Civalek O, Avcar M (2020) Free vibration and buckling analyses of CNT reinforced laminated non-rectangular plates by discrete singular convolution method. Eng Comput. https://doi.org/10.1007/s00366-020-01168-8
46. Lyashenko I, Borysiuk VN, Popov VL (2020) Dynamical model of the asymmetric actuator of directional motion based on power-law graded materials. Facta Univ Ser Mech Eng 18(2):245–254. https://doi.org/10.22190/FUME200129020L
47. Daikh AA, Houari MSA, Belarbi MO, Chakraverty S, Eltaher MA (2021) Analysis of axially temperature-dependent functionally graded carbon nanotube reinforced composite plates. Eng Comput. https://doi.org/10.1007/s00366-021-01413-8
48. Nguyen T-K, Vo TP, Thai H-T (2013) "Vibration and buckling analysis of functionally graded sandwich plates with improved transverse shear stiffness based on the first-order shear deformation theory. Proc Inst Mech Eng Part C J Mech Eng Sci 228(12):2110–2131. https://doi.org/10.1177/0954406213516088
49. Vinh PV (2021) Formulation of a new mixed four-node quadrilateral element for static bending analysis of variable thickness functionally graded material plates. Math Probl Eng. https://doi.org/10.1155/2021/6653350
50. Hassan AH, Kurgan N, Can N (2020) The relations between the various critical temperatures of thin FGM plates. J Appl Comput 6:1404–1419. https://doi.org/10.22055/jacm.2020.34697.2459
51. AlSaid-Alwan HHS, Avcar M (2020) Analytical solution of free vibration of FG beam utilizing different types of beam theories: a comparative study. Comput Concr 26(3):285–292. https://doi.org/10.12989/cac.2020.26.3.285
52. Hadji L, Bernard F, Safa A, Tounsi A (2021) Bending and free vibration analysis for FGM plates containing various distribution shape of porosity. Adv Mater Res 10(2):115–135. https://doi.org/10.12989/amr.2021.10.2.115
53. Hadji L, Avcar M (2021) Free vibration analysis of FG porous sandwich plates under various boundary conditions. J Appl Comput 7(2):505–519. https://doi.org/10.22055/jacm.2020.35328.2628
54. Zenkour AM (2005) A comprehensive analysis of functionally graded sandwich plates: Part 2-Buckling and free vibration. Int J Solids Struct 42(18):5243–5258. https://doi.org/10.1016/j.ijsolstr.2005.02.016
55. Tahir AI, Chikh A, Tounsi A, Al-Osta MA, Al-Dulaijan SU, Al-Zahrani MM (2021) Wave propagation analysis of a ceramic-metal functionally graded sandwich plate with different porosity distributions in a hygro-thermal environment. Compos Struct 269:114030. https://doi.org/10.1016/j.compstruct.2021.114030
56. Rebai B, Bouhadra A, Bousahla AA, Bourada MM, Tounsi A, Tounsi A, Hussain M (2021) Thermoelastic response of functionally graded sandwich plates using a simple integral HSDT. Arch Appl Mech 91:3403–3420. https://doi.org/10.1007/s00419-021-01973-7
57. Bennoun M, Houari MSA, Tounsi A (2016) A novel five-variable refined plate theory for vibration analysis of functionally graded sandwich plates. Mech Adv Mater Struct 23(4):423–431. https://doi.org/10.1080/15376494.2014.984088
58. El Meiche N, Tounsi A, Ziane N, Mechab I, Adda EA (2011) Bedia, "A new hyperbolic shear deformation theory for buckling and vibration of functionally graded sandwich plate." Int J Mech Sci 53(4):237–247. https://doi.org/10.1016/j.ijmecsci.2011.01.004
59. Nguyen V-H, Nguyen T-K, Thai H-T, Vo TP (2014) A new inverse trigonometric shear deformation theory for isotropic and functionally graded sandwich plates. Compos Part B Eng 66:233–246. https://doi.org/10.1016/j.compositesb.2014.05.012
60. Bessaim A, Houari MSA, Tounsi A, Mahmoud SR, Bedia EAA (2013) A new higher-order shear and normal deformation theory for the static and free vibration analysis of sandwich plates with functionally graded isotropic face sheets. J Sandw Struct Mater 15(6):671–703. https://doi.org/10.1177/1099636213498888
61. Pham VV, Le QH (2021) Finite element analysis of functionally graded sandwich plates with porosity via a new hyperbolic shear deformation theory. Def Technol. https://doi.org/10.1016/j.dt.2021.03.006
62. Neves AMA et al (2013) Static, free vibration and buckling analysis of isotropic and sandwich functionally graded plates using a quasi-3D higher-order shear deformation theory and a meshless technique. Compos Part B Eng 44(1):657–674. https://doi.org/10.1016/j.compositesb.2012.01.089
63. Natarajan S, Manickam G (2012) Bending and vibration of functionally graded material sandwich plates using an accurate theory. Finite Elem Anal Des 57:32–42. https://doi.org/10.1016/j.finel.2012.03.006
64. Vinh PV (2021) Deflections, stresses and free vibration analysis of bi-functionally graded sandwich plates resting on Pasternak's elastic foundations via a hybrid quasi-3D theory. Mech Based Des Struct Mach. https://doi.org/10.1080/15397734.2021.1894948
65. Li Q, Iu VP, Kou KP (2008) Three-dimensional vibration analysis of functionally graded material sandwich plates. J Sound Vib 311(1):498–515. https://doi.org/10.1016/j.jsv.2007.09.018
66. Iurlaro L, Gherlone M, Di Sciuva M (2014) Bending and free vibration analysis of functionally graded sandwich plates using the Refined Zigzag Theory. J Sandw Struct Mater 16(6):669–699. https://doi.org/10.1177/1099636214548618
67. Arefi M, Zenkour AM (2017) Size-dependent free vibration and dynamic analyses of piezo-electro-magnetic sandwich nanoplates resting on viscoelastic foundation. Phys B Condens Matter 521:188–197. https://doi.org/10.1016/j.physb.2017.06.066
68. Arefi M, Kiani M, Zamani MH (2018) Nonlocal strain gradient theory for the magneto-electro-elastic vibration response of a porous FG-core sandwich nanoplate with piezomagnetic face sheets resting on an elastic foundation. J Sandw Struct Mater 22(7):2157–2185. https://doi.org/10.1177/1099636218795378
69. Zeng S, Wang BL, Wang KF (2019) Nonlinear vibration of piezoelectric sandwich nanoplates with functionally graded porous core with consideration of flexoelectric effect. Compos Struct 207:340–351. https://doi.org/10.1016/j.compstruct.2018.09.040
70. Daikh AA, Drai A, Bensaid I, Houari MSA, Tounsi A (2020) On vibration of functionally graded sandwich nanoplates in the thermal environment. J Sandw Struct Mater. https://doi.org/10.1177/1099636220909790
71. Salehipour H, Shahidi AR, Nahvi H (2015) Modified nonlocal elasticity theory for functionally graded materials. Int J Eng Sci 90:44–57. https://doi.org/10.1016/j.ijengsci.2015.01.005
72. Batra RC (2021) Misuse of Eringen's nonlocal elasticity theory for functionally graded materials. Int J Eng Sci 159:103425. https://doi.org/10.1016/j.ijengsci.2020.103425